FE Modelling of Mechanical Tensioning for Controlling Residual Stresses in Friction Stir Welds

FE Modelling of Mechanical Tensioning for Controlling Residual Stresses in Friction Stir Welds

D.G. Richards[1], P.B. Prangnell[1], P.J. Withers[1], S.W. Williams[2], A. Wescott[3], E.C Oliver[4]

[1]Manchester Materials Science Centre, UMIST, Grosvenor St. Manchester, M1 7HS, UK.

[2]Cranfield University, Welding Engineering Research Centre, Bedfordshire, MK43 OAL, UK.

[3]BAE Systems, Optics and Laser Technology Department, Advanced Technology Centre, P.O. Box 5, FPC 267, Bristol, BS12 7QW, UK.

[4] ISIS Facility, CCLRC, Rutherford Appleton Laboratory, Chilton, Didcot, OX11 0QX, UK

david.g.richards@postgrad.manchester.ac.uk, philip.prangnell@manchester.ac.uk, philip.withers@manchester.ac.uk,s.williams@cranfield.ac.uk, andrew.wescott@baesystems.com

Keywords: Friction Stir Welding; Residual Stress; FE Modelling; Neutron Diffraction; AA2024.

SYNOPSIS

Although Friction Stir Welding (FSW) avoids many of the problems encountered when fusion welding high strength Al-alloys, it can still result in substantial residual stresses that have a detrimental impact on service life and induce distortion. An FE model has been developed to investigate the effectives of the mechanical tensioning technique for controlling residual stresses in FSWs. The model purely considered the heat input and the mechanical effects of the tool were ignored. Variables, such as tensioning level, heat input, and plate geometry, have been studied. Good general agreement was found between modelling results and residual stress measurements, justifying the assumption that the stress development is dominated by the thermal field. The results showed a progressive decrease in the residual stresses for increasing tensioning levels and, although affected by the heat input, a relatively low sensitivity to the welding variables. At tensioning levels greater than ~ 50% of the room temperature yield stress, tensile stresses were replaced by compressive residual stresses within the weld. Subsequently the modelling has been used to examine how mechanical tensioning can be applied in practical applications.

INTRODUCTION

The development of Friction Stir Welding (FSW), a solid state welding method, has enabled the joining of high strength aluminium alloys that were previously considered unweldable [1]. Although FSW alleviates many metallurgical problems found with fusion welding, such as liquation and solidification cracking, friction stir welds still suffer from similar levels of residual stress, resulting from the weld's local thermal field [2]. High

residual stresses are undesirable due to induced distortion and their effect on mechanical performance. Preliminary work by Williams, *et al* [2, 3] has shown that the application of longitudinal tensioning stress by mechanical stretching during welding can greatly reduce the residual stresses produced the FSW process. In some cases, such as with the application of high levels of mechanical tensioning along the welding direction, the stress state in the weld can actually be reversed, so that compressive residual stresses are formed [3]. Studies have been performed on the effectiveness of this method for controlling residual stresses in FSWs [4] but work has concentrated on the effect of the level of tensioning applied. Much modelling work has been carried out on the FSW process (e.g. [4-12]) and there have been a few models developed to predict the residual stresses generated. However there has been little, or no, modelling into the combined effects of welding stress development and mechanical tensioning.

In order to improve current understanding of the potential of mechanical tensioning, for controlling residual stresses in FSW airframe structures, a simplified FE model has been developed to simulate the process. The approach used and results from the model are presented in this paper. The model output is compared with previously obtained/published experimental data that was measured by x-ray synchrotron diffraction at ESRF-ILL [13], and from subsequent calibration measurements made on further samples at ISIS-RAL using neutron diffraction as part of this investigation.

ORIGINAL FE MODEL AND HEAT SOURCE CALIBRATION

The modelling approach adopted was based on the work of Q. Shi, *et al* [9] and M. Peel [14] and relied purely on the thermal field generated by the welding tool. The metal flow and mechanical effects of the tool were not considered. This simplification is computationally very helpful and has previously been found to give good results, as the formation of residual stresses in FSW is normally dominated by the heat input [9, 11, 12, 15, 16]. The model was implemented in ABAQUS using a standard sample plate geometry of 1135 x 250 x 3mm that replicated the test coupons and clamping used to produce supporting experimental data at BAE Systems, ATC, Filton. The model comprised a single partitioned plate, representing the two separate plates to be welded, the partition line being along the weld line. A graded mesh was used with 1mm x 1mm x 3mm elements at the weld line, which increased to 25mm x 25mm x 3mm at the edge of the plate. The plate was pinned vertically along its length at 40mm from the weld line to simulate clamping and the tension force was applied uniformly along one edge normal to the welding direction. The material and thermal-physical properties used were for a standard AA2024 alloy [17]. The FSW heat source was simulated by using a circular surface source, to represent the tool shoulder (Q_s), and a cylindrical volume source, to represent the tool pin (Q_p), which were traversed along the weld line using an ABAQUS subroutine. The distribution of the heat flux under the tool shoulder, q_s, at a radius, r, was assumed to be linear with angular velocity, based on the work of Y.J. Chao, *et al* [4, 5]; given by:

$$q_s(r) = \frac{3}{(2p)} \frac{Q_s r}{\left(R_s^3 - R_p^3\right)} \quad (1)$$

Where R_s and R_p are the dimensions of the shoulder and pin. The heat input from the pin was assumed to be uniform with the pin depth and was assigned to be 12% of the total power, based on previous experience [4, 5, 7, 15, 16] and calibration studies, with the remainder distributed under the shoulder. Heat loss was simulated using artificial surface convection coefficients [18] for each surface boundary condition to simulate conduction to the welding base-plate, retaining clamps, and to air. This method allowed the jigging parts to be omitted from the model, saving on simulation times. The thermal profile generated by the thermal model was used as an input to the mechanical model in the form of nodal temperatures.

Calibration of the heat source and surface convection coefficients was achieved by matching thermal profiles, captured by an infrared thermal imaging camera obtained during the creation of the FSW test coupons, to the model output. The standard welding condition used was 770rpm and 195mm/min. Several successive model simulations were run until a reasonable match was obtained, resulting in a shoulder power input, Q_s, of 1120W and a pin power input, Q_p, of 120W, giving a total power input of 1240W, to represent the welding parameters of 770rpm and 195mm/min. This calibration method allowed the heat loss through the tool to be ignored (i.e. the actual tool power would be ~ 40% higher). The thermal profile generated by this power input was then used for the simulated tensioning experiments. The heat input was subsequently systematically varied around this value within the constraints of the material melting and the temperature becoming unrealistically low.

RESULTS AND DISCUSSION

Effect of Mechanical Tensioning Under Standard Welding Conditions

In welding, as the heat source advances, material ahead of the source expands and develops compressive stress, because it is constrained by the colder surrounding material. This stress largely plastically relaxes (compressive yielding) due to the low material yield stress at high temperatures [13, 19]. The contracting hot metal behind the heat source thus develops a misfit strain as it cools, resulting in a tensile residual stress that is maximum in the welding direction and is balanced by a small far field compressive stress in the plate. If tensile yielding occurs in the soft material cooling behind the weld then a reduction in tensile stresses occurs on the weld centreline and the resultant residual stress profile has the characteristic ‘M’ shape. Mechanical tensioning has two effects:

1. The tensile stress reduces the amount of compressive yielding that occurs ahead of the weld (reduced compressive yielding – RCY). This leads to a reduction in the size of the tensile residual stress that is produced on cooling and can eliminate it all together.
2. The increased tensile stress level also leads to increased relaxation of the developing tensile residual stress in the cooling material behind the weld (induced tensile yielding – ITY). After unloading the ITY leads to a compressive residual stress profile which is superimposed on the tensile residual stress profile

produced by the compressive yielding ahead of the weld. If the RCY has been sufficient to eliminate this tensile residual stress then the overall result including the ITY is a band of compressive stresses across the weld zone.

To investigate how effective this technique can be, mechanical tensioning loads were applied in the model simulations during welding, under the standard condition with the fitted heat source, using tensioning stress levels defined in terms of the percentage of the room temperature yield stress for AA2024 (325MPa). Examples of predicted longitudinal residual stress distributions from the model, in the plane of the plate surface, with and without any mechanicaltensioning, are shown in Fig. 1a. Without tensioning the modelled stress distribution indicates a maximum tensile residual stress of 184MPa that occurs symmetrically and corresponds approximately with the edge of the tool shoulder, giving the M-shaped profile described previously. With an applied mechanical tensioning load of 35% of yield stress the residual stress profile after unloading is almost zero. For a higher level of applied mechanical tensioning the residual stress after unloading comprises a band of compressive stresses across the weld zone. There are small balancing tensile stresses away from the weld zone.

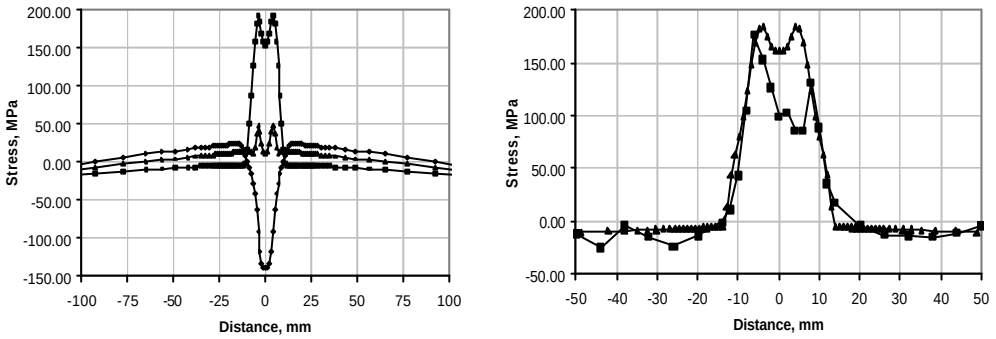

Fig. 1. Longitudinal stresses in (a) predicted from the model for an un-tensioned and tensioned (to 35% and 70% of yield stress) AA2024 plate, and in (b), a prediction for a 10% tensioned plate compared to one measured by neutron diffraction. All using a heat input of 1240W representing the welding parameters of 770rpm and 195mm/min.

As part of the investigation a calibration comparison was made using measurements obtained by neutron diffraction at ISIS-RAL, using an AA2024, 780 x 400 x 3mm, FSW sample that had been tensioned by 10% during welding under nearly identical conditions of 770rpm and 200mm/min to the calibrated heat source used in the model. The longitudinal stress profile from these measurements is compared in Fig. 1b with modelling predictions for the same tensioning level. It can be noted from this figure that the model profile gives a very good reproduction of the measured profile, but the stresses are slightly over estimated, with values of 184MPa, compared to 176MPa for the measured results. The asymmetry in the measured weld profile is due to the effects of the advancing and retreating sides of the tool. This is not taken into account in the model.

While in future work it is planned to measure residual stresses in coupons produced with identical geometry and welding conditions, in the short term preliminary experimental data was sought to verify these predictions. A comparison was therefore made with data provided by Price, *et al* [13] for the same geometry as the model,

showing the effect of tensioning on the peak longitudinal stresses in AA2024 1m long welds determined from x-ray synchrotron diffraction measurements, with welding conditions of 350rpm and 195mm/min. All of these results are depicted together in Fig. 2a, with the measured data giving similar trends to the model simulations, despite the different welding conditions.

Effect of Varying the Tool Heat Input Power

Simulations were carried out to determine the effect on the residual stress distribution, at different tensioning levels, of changes in the heat input, which would result from altering the tool RPM. Total power input values of 960W, 1442W, and 1560W were selected to compare to the original total tool power of 1240W. The peak stress levels that result from these simulations are shown in Fig 2b. Without tensioning, the higher heat input results in slightly higher maximum residuals stresses. As the tensioning level is increased and the residual stress becomes compressive, the curves cross and the higher heat input curves have a higher level of compressive stress. It can be seen that if a zero residual stress level is required the applied mechanical tensioning level varies with heat input, with higher levels needed for higher heat inputs

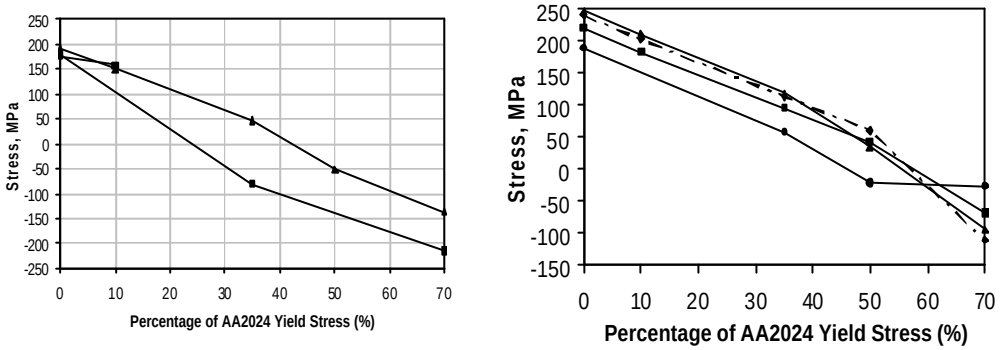

Fig. 2. Predicted values of maximum longitudinal residual stress, as a function of tensioning level, in terms of percentage of the yield stress, under the standard welding condition of 770rpm and 195mm/min, in (a) compared to three measured samples with similar welding conditions, and data taken from Price, *et al* [13] using 350rpm and 195mm/min; and in (b) results for simulated power inputs of 960W, 1240W, 1442W and 1560W for AA2024 (standard geometry).

Varying the Tool Traverse Speed

As an additional form of investigation, the standard power input of 1240W applied to the standard plate geometry at 195mm/min was now supplemented by altering the traverse speed to 100mm/min and 300mm/min. With the same model and boundary conditions being used in each case, only the speed at which the heat source traversed the weld was varied, resulting in a change to the amount of heat applied to the weld. The results of this study are shown in Fig. 3.

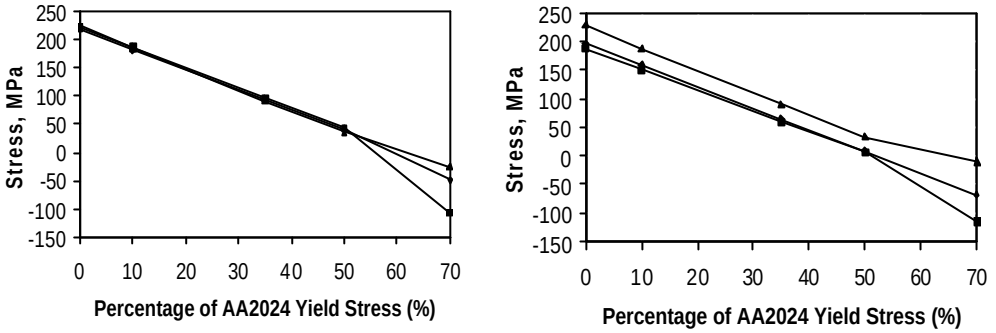

Fig. 3. Predicted values of longitudinal residual stress, as a function of tensioning level, in terms of percentage of the yield stress, using the standard welding input power of 1240W for the AA2024 standard plate geometry, and for 100, 195 and 300mm/min traverse speeds, in (a) maximum peak values at the edge of the weld; and in (b) minimum trough values at the centre of the weld.

For the three traverse speeds of 100, 195, and 300mm/min, the resulting peak weld temperatures produced by the model were 455°C, 428°C, and 393°C respectively. In Fig. 3a it can be seen that there is very little difference between the peak residual stresses at the edge of the weld for all three traverse speeds for tensioning levels below 50% of the yield stress. Above this point a decrease in speed leads to an increase in compressive residual stress level. This is because the compressive stresses are produced by ITY behind the weld and the level of this yielding is higher for hotter welds. Figure 3b shows the effect of the travel speed on the stress level at the centre of the weld where the ITY occurs. It can be seen that the level of ITY and hence the resultant residual compressive stress is higher for slower, hotter welds.

Asymmetric Welds and Non-Rectangular Plate Geometries

For practical applications it may not always be possible to apply the tensioning parallel to the weld direction and the plates to be welded may not have a rectangular profile. Therefore the effect of asymmetric welds and geometries was also investigated by the creation of a model comprised of a rectangular plate geometry, but with a weld that was zero, six, twelve and twenty degrees off-axis from the centre line (the angular rotation of the weld being centred on the centre of the plate – see Fig. 4). The predicted longitudinal residual stress distributions for these simulations are shown in Fig. 5. It can be seen that as the angle is increased at the higher tensioning levels a marked asymmetry in the residual stress profile is produced. For the application of interest the angle required is six degrees and in the case the asymmetry is not sufficient to cause a problem.

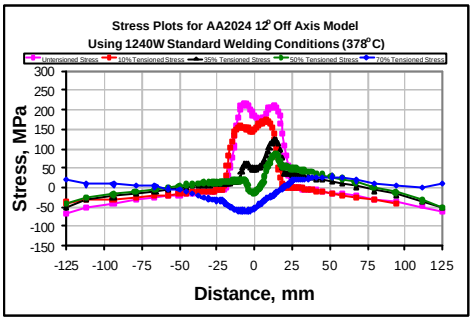

(c) (d)

Fig. 5. Predicted longitudinal residual stress profiles for various mechanical tensioning loads with the tensioning applied at (a) zero, (b) six, (c) twelve and (d) twenty degrees to the weld centreline using the standard welding input power of 1240W and 195mm/min traverse speed for the AA2024 standard plate geometry.

A final investigation was carried out on a model comprising of a standard plate modified by tapering each side parallel to the weld line by 6°. The weld was along the centreline as normal. Predicted values of maximum longitudinal residual stress normalised over the length of the plate are shown in Fig. 6. The results show that the tensioning effect is not greatly influenced by the global plate geometry, as the peak stresses along the length of the weld are reduced in line with previous results for the parallel-sided standard plate, thereby indicating that the peak stresses are most influenced by the local tensioning applied at that point in the weld.

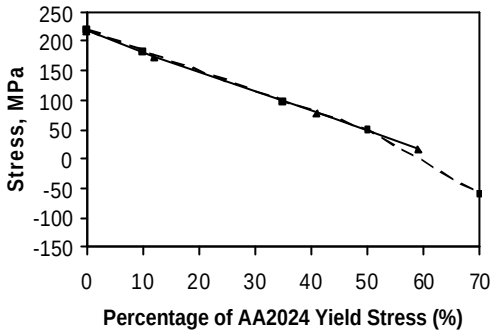

Fig. 6. Predicted values of maximum longitudinal residual stress, as a function of tensioning level, in terms of percentage of the yield stress, for the AA2024 standard plate compared with a 6^{o} tapered plate geometry. All using the standard welding input power of 1240W and 195mm/min traverse speed.

The effect of different weld geometries was also investigated by the creation of a model comprising a far shorter plate measuring 350mm x 250mm x 3mm, using the same tensioning range and power input (1240W). The peak residual stresses were compared to the original model results and gave a very similar behaviour. The above analysis thus suggests that, in terms of the peak residual stresses, the most dominant parameter is the applied tensioning level and that the mechanical tensioning process is very robust.

CONCLUSIONS

The residual stress model developed, based purely on the FSW tool thermal field, showed reasonable agreement with published data and a calibration sample measured by neutron diffraction. The model proved to be a good tool for the investigation of the effectiveness of mechanical tensioning for controlling residual stresses in FSW's. The simulations and measurements showed a progressive decrease in the residual stresses with increasing tensioning applied during welding. This continued until 50% of the yield stress at room temperature was exceeded, at which point the tensile stresses in the weld were eliminated and replaced by increasing levels of compressive stresses. Comparisons between different power inputs and traverse speeds (representing different welding parameters), and different plate geometries all produced consistent results, and showed that the peak stresses, although influenced by the heat input, were not dramatically affected by the welding conditions.

The model was used to investigate the application of mechanical tensioning in a real industrial application. Here the load has to be applied at an angle to the weld centerline and the welds plates are tapered. The model showed that the effect of the angle was to cause an asymmetry in the residual stress profile but that this would not be a problem for the required case of six degrees. The model showed that tapered shape of the plates to be welded had no effect on the performance of the mechanical tensioning system.

ACKNOWLEDGEMENTS

This work is supported through the University of Manchester EPSRC Light Alloys Portfolio Partnership (EP/D029201/1) in collaboration with Airbus UK.

REFERENCES

1. Thomas, W.M. and E.D. Nicholas: *Friction stir welding for the transportation industries*. Materials and Design, 1997. **18**(4-6): p. 269-273.
2. Staron, P. and M. Kocak, S.W. Williams and A. Wescott: *Residual stress in friction stir-welded Al sheets*. Physica B: Condensed Matter, 2004. **Volume 350** (Issues 1-3, Supplement 1), 2004. p. Pages E491-E493.
3. Williams, S.W., D.A. Price., A. Wescott, C.J.C. Harrison, P. Staron and M. Kocak: *Distortion Control in Welding by Stress Engineering*. BAe Systems, 2004
4. Williams, S. W. D.A. Price, A. Wescott, A. Steuwer, M.Peel, J.Altenkirch, P.J.Withers, and M.Poad: *Distortion Control in Welding by Mechanical Tensioning.* (These proceedings)
5. Chao, Y.J., X. Qi, and W. Tang: *Heat Transfer in Friction Stir Welding - Experimental and Numerical Studies*. Journal of Manufacturing Science and Engineering, 2003. **125**(1): p. 138-145.
6. Song, M. and R. Kovacevic: *Thermal Modelling of Friction Stir Welding in a Moving Coordinate System and its validation*. International Journal of Machine Tools and Manufacture, 2003. **43**(6): p. 605-615.
7. Tang, W., X.G., J.C. McClure, and L.E. Murr: *Heat Input and Temperature Distribution in Friction Stir Welding*. Journal of Materials Processing & Manufacturing Science, 1999. **7**(2): p. 163 172.
8. Ulysse, P: *Three-dimensional Modelling of the Friction Stir-WeldingPprocess*. International Journal of Machine Tools and Manufacture, 2002. **42**(14): p. 1549-1557.
9. Shi, Q. and T. Dickerson and H.R. Shercliff: *Thermo-Mechanical FE Modelling of Friction Stir Welding of Al-2024 Including Tool Loads*. 4th International Symposium on FSW (cd rom), Utah, USA, TWI, 2003.
10. Chen, C.M. and R. Kovacevic: *Finite Element Modelling of Friction Stir Welding -Thermal and Thermomechanical Analysis*. International Journal of Machine Tools and Manufacture, 2003. **43**(13): p. 1319-1326.
11. Colegrove, P.A: *3 Dimensional Flow and Thermal Modelling of the Friction Stir Welding Process.* Dissertation in Department of Mechanical Engineering, University of Adelaide, 2001.
12. Colegrove, P.A. and H.R. Shercliff: *Determining the Heat Generation in Friction Stir Welding from Simplified Flow Models*. Cambridge. p. Draft document, 2005.

13. Price, D. and C.J. Harrison, S.W. Williams, A. Wescott, A. Johnson, J. Gabzdyl, M. Smith and M. Rahim: *The Performance of Active Tensioning Techniques for Stress Control in Welding*. BAe Systems Report No JS 15232, 2004.
14. Peel, M.J: *The Friction Stir Welding of Dissimilar Aluminium Alloys*. Dissertation in School of Materials, University of Manchester, Manchester, 2005.
15. Colegrove, P.A., M. Painter, D. Graham and T. Miller: *3 Dimensional Flow and Thermal Modelling of the Friction Stir Welding Process*. 2nd International Symposium on FSW (cd rom), Gothenburg, Sweden, 1999.
16. Colegrove, P.A. and H.R. Shercliff: *3-Dimensional CFD modelling of flow round a threaded friction stir welding tool profile*. Journal of Materials Processing Technology, 2005. p. In Press, Corrected Proof.
17. Harrison, C.J: *Material Properties Summary*. European Union 5th Framework Project (WAFS), BAE Systems, 2004.
18. QinetiQ. Internal Report, 2005.
19. Masubuchi, K: *Analysis of Welded Structures*. Oxford, Pergamon Press, 1980.